Motion and vision. II. Stabilized spatio-temporal threshold surface

D. H. Kelly

SRI International, Menlo Park, California 94025

(Received 16 February 1979; revised 25 May 1979)

The stabilized contrast-sensitivity function measured at a constant retinal velocity is tuned to a particular spatial frequency, which is inversely related to the velocity chosen. The Fourier transforms of these constant-velocity passbands have the same form as retinal receptive fields of various sizes. At low velocities, in the range of the natural drift motions of the eye, the stabilized contrast-sensitivity function matches the normal, unstabilized result. At higher velocities (corresponding to motions of objects in the environment), this curve maintains the same shape but shifts toward lower spatial frequencies. The constant-velocity passband is displaced across the spatio-temporal frequency domain in a manner that is almost symmetric about the constant-velocity plane at $v = 2$ deg/s. Interpolating these diagonal profiles by a suitable analytic expression, we construct the spatio-temporal threshold surface for stabilized vision, and display its properties in terms of the usual frequency parameters; e.g., at low spatial frequencies, the temporal response becomes nearly independent of spatial frequency, while at low temporal frequencies, the spatial response becomes independent of temporal frequency.

INTRODUCTION

In the first paper of this series,[1] we described a noncontact method of accurately stabilizing the retinal image, which has certain advantages over contact-lens methods. Here we make use of this technique to explore spatio-temporal interactions in the visual system, without the artifacts introduced by uncontrolled eye movements.

One way to measure these interactions in the steady state involves a stimulus configuration that was suggested almost 20 years ago,[2–4] combining the sine-wave flicker stimuli of DeLange[5] and the sine-wave grating patterns of Schade[6] to produce counterphase, flickering gratings.[7] Several years after these combined stimuli were first proposed, they were used in (unstabilized) threshold measurements by Kelly[8] and Robson[9] independently.

If we regard the counterphase grating as a small perturbation $f_S(x,t)$ superimposed on a large, steady background, then it can be treated as a standing wave, and factored into independent spatial and temporal components. Thus,

$$f_S(x,t) = \cos\alpha x \cos\omega t = f_1(x)f_2(t), \qquad (1)$$

where $f_1(x) = \cos\alpha x$, and $f_2(t) = \cos\omega t$. In the absence of spatio-temporal interaction in the visual process, we would expect the spatial and temporal *responses* to be separable in the same way.[4] That is, the shape[10] of the flicker sensitivity curve should be independent of the spatial frequency α at which it is measured, and the shape of the contrast sensitivity curve should be independent of the temporal frequency ω at which it is measured. But that is not the case. Both early studies[8,9] found that the spatio-temporal threshold surface is not separable; it cannot be constructed by multiplying together a standard contrast threshold curve and a standard flicker threshold curve.

Similar measurements[11] have also been made with a closely related stimulus configuration, of the form

$$f_T(x,t) = \cos\alpha(x - vt). \qquad (2)$$

This expression represents a grating of spatial frequency α, drifting across the visual field at velocity v. Since $v = \omega/\alpha$, where ω is the temporal frequency at a fixed point in space, the stimuli of Eqs. (1) and (2) are related by a well-known trigonometric identity,

$$2\cos\alpha x \cos\omega t = \cos\alpha(x - vt) + \cos\alpha(x + vt), \qquad (3)$$

i.e., a standing wave can be regarded as the sum of two traveling waves, moving in opposite directions at the same speed. Each of these traveling components contributes half of the standing-wave amplitude (as measured at an antinode).

With traveling-wave stimuli,[12] Van Nes *et al.*[11] measured unstabilized thresholds that were qualitatively similar to the standing-wave thresholds of Robson[9] or Kelly.[8] However, no quantitative comparisons of these two types of experiments were attempted until 1975, when Levinson and Sekular,[13] again using unstabilized stimuli, made a direct comparison of the psychophysical sensitivity to drifting and flickering gratings, with the same apparatus, same conditions, and same subject for both experiments. They found motion sensitivity to be consistently greater than flicker sensitivity. Indeed, their data suggested that, at least over a limited range of spatial and temporal frequencies, the traveling-wave and standing-wave threshold surfaces may have the same shape, differing only by a factor of 2. If this result holds over a large region of the spatio-temporal frequency domain, it has important consequences.

In any case, the fact that motion thresholds are lower than flicker thresholds suggests that moving gratings are somehow better matched to the characteristics of the visual process than are flickering gratings. Because of the equivalence of a standing wave and the sum of two half-amplitude traveling waves [see Eq. (3)], Levinson and Sekular[13] interpreted their measured factor of 2 as evidence for independent, direction-sensitive mechanisms in the brain. Regardless of the mechanism involved, however, any constant ratio between the two thresholds would simplify our theoretical modeling of spatio-temporal interaction: A model that explained the shape of one surface might then be able to explain both.

Since all the studies described above were conducted without stabilization of the retinal image, any explanation of their results in terms of neural mechanisms may be confounded by the effects of involuntary eye movements on the retinal input. It has now been shown that eye movements

 0030-3941/79/101340-10$00.50

have profound effects on the thresholds for stationary gratings[1,14] and smaller, but still significant, effects on the thresholds for flickering gratings.[14] In this paper, we study the thresholds for stabilized, drifting gratings over the entire spatio-temporal frequency domain.

If the traveling wave is a more fundamental stimulus than the standing wave, then perhaps velocity is a more fundamental parameter than temporal frequency. Measuring the contrast sensitivity at several fixed velocities, we obtain broadly tuned bandpass curves of contrast sensitivity, each peaking at a spatial frequency that depends on the velocity chosen. In log-log coordinates, these curves all have approximately the same shape, resembling the Fourier transform of a receptive-field function. When the stabilized velocity equals the drift velocity of the subject's natural eye movements, the resulting curve matches the peak of his normal, unstabilized contrast sensitivity (but is slightly narrower).

The standard shape of the constant-velocity curves simplifies our search for an analytic description of the spatio-temporal threshold surface over the usual range of spatial and temporal frequencies. Here we construct the surface by interpolating between these constant-velocity, diagonal profiles (instead of the constant-frequency profiles, which vary in shape). Since the standing-wave threshold at any point is twice the traveling-wave threshold, the same description also applies to the threshold surface for counterphase-flickering gratings.

I. METHODS

For details of our eyetracking and stabilization apparatus, calibration, and psychophysical procedures, the reader is referred to Part I of this series.[1] Our stimulus pattern was a stabilized, 300-td, neutral gray, vertical, flickering or drifting, sine-wave grating, which filled an unstabilized 7.5° circular aperture. Unstabilized fixation marks were also provided. The subject adjusted the contrast of the stabilized pattern to his threshold, waited a few seconds (to be sure his response represented the steady state), then pressed a button to call for a new spatial frequency (or velocity, or both).

The previous paper[1] reported several comparisons of stabilized and unstabilized thresholds for stationary gratings. It was shown that our stabilizer is precise enough to elevate the threshold for a 3 c/deg grating by a factor of 20, which is an order of magnitude greater than the threshold elevations reported for other stabilization methods. Since it requires no contact with the eye, our technique permits lengthy experiments if desired.

In this paper, we abandon unstabilized stimuli. When we want the image to move across the retina, we impose the desired motion at the object, where we can control it. Thus all the data presented here were obtained under stabilized conditions (except for the points in Fig. 7).

II. THRESHOLDS FOR STANDING AND TRAVELING WAVES

Does the spatio-temporal threshold surface have the same shape for traveling waves that it does for standing waves? To answer that question, we compared these two types of stimuli,

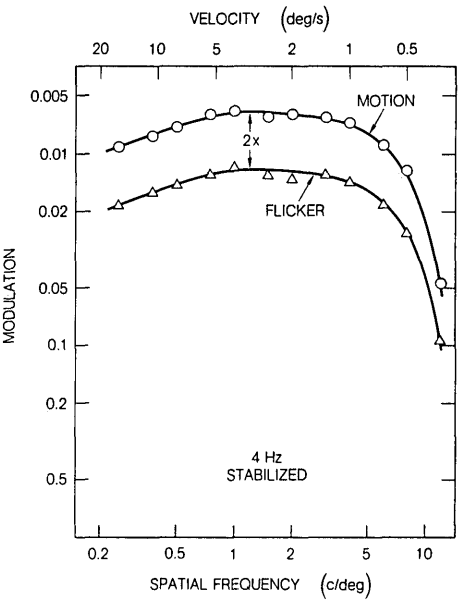

FIG. 1. Stabilized contrast-sensitivity measurements, at a constant flicker rate of 4 Hz, with standing (triangles) and traveling (circles) waves. The template curves are separated by a ratio of 2.0. Traveling-wave velocities are shown at the top of the figure. Circular field, 7.5° in diameter, 300 td, 2.3-mm artificial pupil.

as Levinson and Sekular[13] did, but over a greater range of spatial and temporal frequencies, and with stabilization of the retinal image throughout our experiments. Some typical results are given in Figs. 1–4.

Figure 1 shows the two contrast-sensitivity profiles parallel to the spatial-frequency axis at a temporal frequency of 4 Hz. The standing-wave and traveling-wave modulation thresholds are defined in the same way as in the previous studies discussed above.[8,9,11,13] The two template curves in the figure are separated by a factor of exactly 2.0. None of the data departs significantly from these curves.

Figure 2 shows another pair of contrast-sensivitity profiles, measured at 12 Hz; the factor of 2 holds here as well. To keep the temporal frequency constant in these experiments, the velocity must be varied in accord with relation, $\alpha = \omega/v$. The resulting velocity scales are shown at the top of each figure. [The velocities for the standing waves are defined by Eq. (3).]

Note that the template curve in Fig. 2 is not the same one we used in Fig. 1. As will be shown below, these changes of curve shape do not occur when each curve is measured at a constant velocity. Also, neither template resembles the unstabilized contrast-sensitivity curve for stationary gratings.[1] In fact, there is no constant temporal frequency that simulates the unstabilized contrast sensitivity very well. That requires a constant velocity, as discussed below.

Figure 3 shows another pair of sensitivity profiles, this time parallel to the temporal frequency axis, at a spatial frequency of 1 c/deg. To keep the spatial frequency constant, again the velocity must vary, in this case directly with the temporal frequency, as shown by the scale at the top of the figure. The motion sensitivity still seems to be exactly twice the flicker sensitivity in this region of the threshold surface.

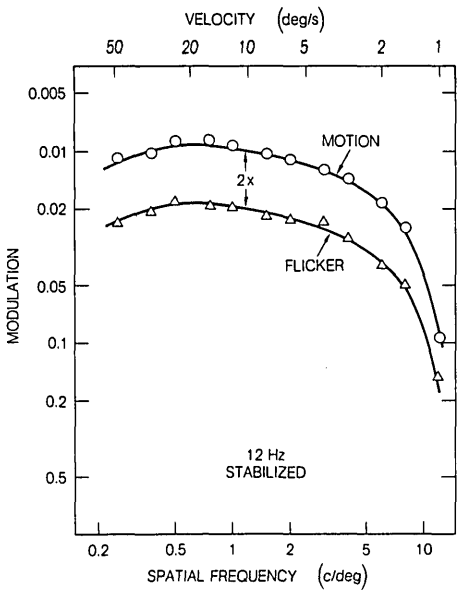

FIG. 2. Same as Fig. 1, but at a constant flicker rate of 12 Hz. The traveling-wave velocities, and the shape of the template curve, are also different from those of Fig. 1.

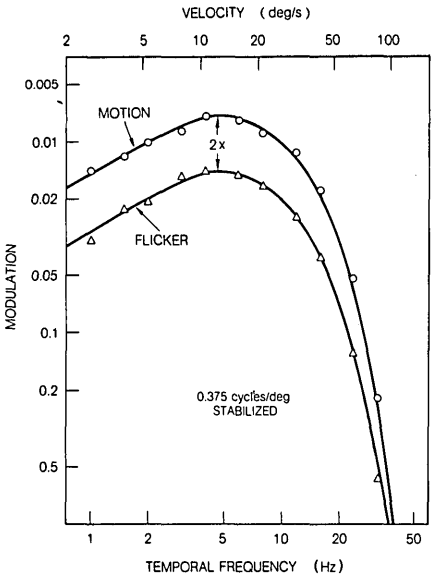

FIG. 4. Same as Fig. 3, but at a fixed spatial frequency of 0.375 cycles/deg. At this low spatial frequency, the shape of the template is beginning to resemble the standard (wide-field) flicker curves.

We have not measured the ratio of motion to flicker sensitivity for every possible combination of spatial and temporal frequencies, but we have sampled the spatio-temporal frequency domain widely enough to be convinced that both stabilized threshold surfaces have the same shape, at least over the range of spatial and temporal frequencies usually studied.[8,9,11,15] This occurs even at very low spatial frequencies, where we might expect it to break down.[16] For example, Fig. 4 shows the profiles obtained at 0.375 c/deg, where only three waves fill our stimulus field. Although the template curve is beginning to resemble the flicker sensitivity for a uniform field,[15] all parts of this stimulus pattern are evidently still interacting to yield the ratio of 2.0.

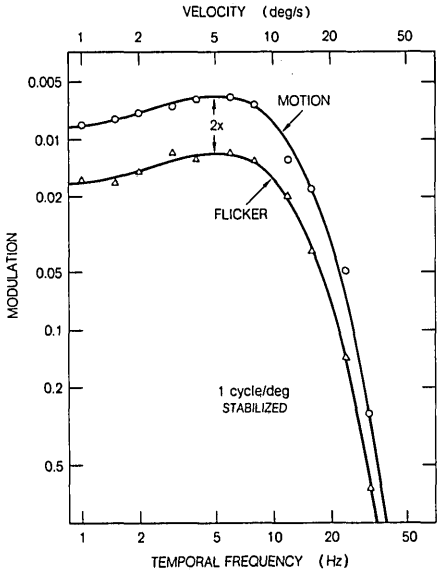

FIG. 3. Stabilized flicker-sensitivity measurements with standing (triangles) and traveling (circles) waves at a fixed spatial frequency of 1 cycle/deg. Traveling-wave velocities are shown at the top of the figure. The template curves are separated by a ratio of 2.0.

To test further the relation between standing and traveling waves, we also performed an experiment in which the two stimuli were combined. A counterphase-flickering grating was moved across the field at the velocity of one of its traveling components, as defined by Eq. (3), resulting in a stimulus of the form,

$$f_{ST}(x,t) = \cos\alpha(x - vt)\cos\omega t$$
$$= (1/2)\cos\alpha x + (1/2)\cos\alpha(x - 2vt).$$

Now, if $v = \omega/\alpha$ exactly, then one of the traveling components becomes stationary, neither moving nor flickering, while the other moves across the field with twice its normal velocity.[17] Under these conditions, only the moving component should be detected, because the threshold for the stationary component would be much higher.[1]

Figure 5 shows the results of such an experiment, at a spatial frequency of 0.375 c/deg, as a function of temporal frequency. The corresponding velocities are again given at the top of the figure. The dashed curve is the traveling-wave sensitivity, reproduced from Fig. 4. The right-angle arrow represents the two predictions that follow if only the moving component is detected: (a) the template curve should be moved one octave lower in temporal frequency (relative to ω); and, (b) all threshold contrasts should be doubled. The data obey prediction (a) exactly, but the thresholds are all about 10% greater than predicted. That small but significant discrepancy is due probably to residual eye-movement effects that were unavoidable in this particular test.[17]

With good stabilization, we can evidently abandon standing waves in favor of traveling waves without losing any information, because we can obtain any stabilized, standing-wave threshold over most of the spatio-temporal frequency domain, merely by doubling the corresponding traveling-wave threshold. Our data suggest that eye movements were the cause of previous occasional failures[13,18] to obtain this ratio of 2.0. With poor stabilization, the two thresholds move closer

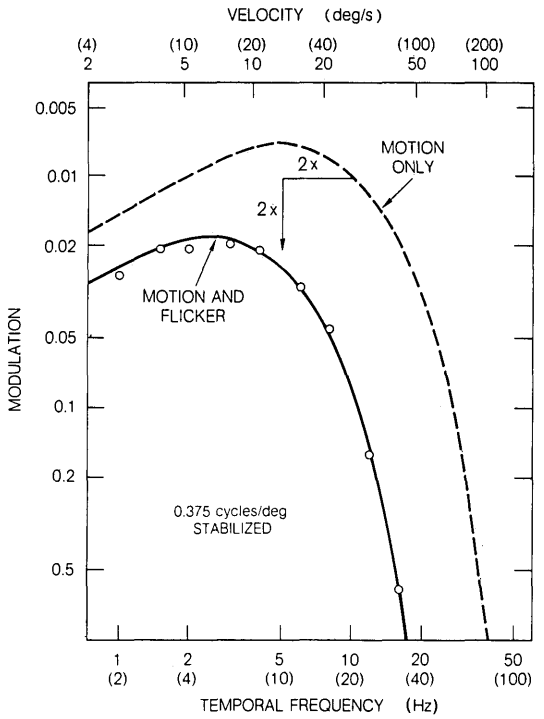

FIG. 5. Sensitivity to a standing-wave stimulus that is being moved at a velocity that just cancels the velocity of one of its traveling-wave components. This procedure doubles the velocity (and hence the temporal frequency) of the other traveling component, as indicated by the numbers in parentheses. The dashed curve is copied from Fig. 4 for comparison. The solid curve shows the same template, translated one octave in frequency, and adjusted vertically to fit the data.

together, probably because natural eye movements increase the standing-wave sensitivity at most frequencies, as we have shown elsewhere.[14]

Qualitatively, it is easy to see why the traveling wave is the more effective stimulus: It provides equal modulation at every point in the stimulus field (as Van Nes *et al.*[11] first pointed out). The stabilized standing wave, by comparison, has no temporal variation at its nodes and less modulation everywhere except at its antinodes. (The reason eye movements increase the standing-wave sensitivity[14] is probably that they move the nodes around, so there are no completely unstimulated regions of the visual field.) Perhaps the stabilized traveling wave is, in some sense, the optimum spatiotemporal stimulus, reflecting certain fundamental properties of the visual pathways.

III. CONTRAST SENSITIVITY AT CONSTANT VELOCITY

From our present viewpoint, earlier measurements of contrast sensitivity at a constant flicker rate (including Figs. 1 and 2 above) represent an unnatural situation, because every spatial frequency is tested at a different velocity. When natural eye movements translate a real visual scene across the retina, on the other hand, every Fourier component of that scene moves *at the same velocity.* Thus it is not unreasonable to suppose that we would learn more about how the retina normally resolves these traveling components if we held the velocity constant while measuring the contrast sensitivity.

Figure 6 shows six stabilized contrast-sensitivity curves measured in this way, at velocities ranging from 0–32 deg/s. They are, of course, profiles across the same threshold surface crossed by the upper curves in Figs. 1–4, but these constant-velocity data represent diagonal paths across that surface. The curves in Fig. 6 were simply drawn through the points without attempting to maintain a constant shape. In Sec. IV, however, we will show that for velocities greater than 0.1 deg/s, these curves can be fitted almost equally well by a common template (previously used to model the unstabilized contrast sensitivity).[19] Any fixed velocity in Fig. 6 seems to extract a subset of broadly tuned retinal units, which peak at higher spatial frequencies as the velocity decreases.

At velocities much less than 0.1 deg/s, the overall sensitivity drops gradually down toward the level obtained with a stationary, stabilized grating. Even at a retinal velocity of only one or two foveal cone cells per second (filled symbols in Fig. 6), the sensitivity is still four times greater than the zero-velocity curve over a wide frequency range. For this and other reasons,[20] we speculate that the zero-velocity curve may represent a fundamental limit to the fading of stabilized images; perhaps it is mediated only by receptive fields that respond to sustained stimulation.

Similar constant-velocity experiments were conducted by Watanabe *et al.*[21] without stabilizing the retinal image. As might be expected, they found no loss of sensivitivy at very low stimulus velocities, but at higher velocities they obtained a spatial tuning effect qualitatively similar to that shown in Fig. 6. In another unstabilized experiment, Arend[22] obtained a similar tuning effect with stationary gratings by instructing the subject to follow a fixation point that moved across the grating at a constant velocity. We, therefore, infer that this

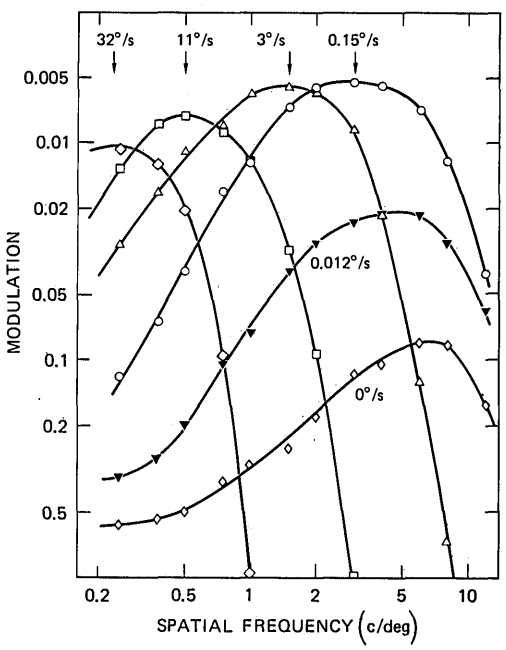

FIG. 6. Stabilized contrast-sensitivity curves measured at constant velocity. Data are shown for six different velocities, ranging from 32 deg/s down to zero. Note that the curve shape remains essentially constant for all velocities greater than about 0.1 deg/s. The curve for 0.012 deg/s (filled symbols) represents a retinal velocity of about two cone cells per second.

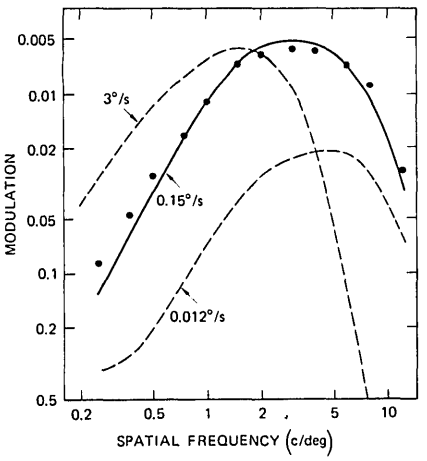

FIG. 7. Points representing the normal, unstabilized contrast sensitivity of the same subject as in Fig. 6, from which the three smooth curves are copied. These unstabilized data are best fitted by the stabilized constant-velocity result for 0.15 deg/s (solid curve).

velocity tuning behavior also occurs in normal, unstabilized vision. Our procedure merely provides a more precise method for measuring it.

Although Fig. 6 shows only six samples across our tuning range, the peak of the contrast sensitivity curve can, of course, be set at any intermediate spatial frequency, merely by choosing the appropriate velocity. This continuum runs from the low-velocity region in which the sensitivity level changes rapidly but the peak frequency does not, to the high-velocity region in which the peak frequency changes rapidly but the sensitivity level does not.

Between those two extremes, however, there is a wide range of velocities where the contrast sensitivity curve is relatively immune to both effects. The data at 0.15 deg/s (open circles in Fig. 6) fall within this region in which the curve shifts very slowly with changing velocity. Since this is also the velocity range of the subject's normal drift motions, it can scarcely be a coincidence that the 0.15 deg/s curve closely resembles the normal, unstabilized contrast sensitivity.

One of the goals of the present study was to find "...the particular condition of stabilized motion with which we can duplicate the normal, unstabilized contrast sensitivity function for stationary gratings."[1] To show how closely this goal has been achieved, in Fig. 7 we compare the stabilized curves for three different velocities with the unstabilized contrast thresholds for the same subject. We can almost match the natural contrast sensitivity function by moving the stabilized retinal image at the appropriate velocity. The velocity that is closest to the subject's natural drift velocities provides the best fit, but the bandwidth of the natural sensitivity data is slightly broader than the single-velocity curve, suggesting that the unstabilized threshold data represent a considerable range of drift velocities.

If further proof were needed that the natural drift motions mediate normal vision, this seems to provide it. To the extent that the sine-wave contrast-sensitivity curve represents the properties of pattern vision in general, those properties can be simulated by superimposing, on the stabilized retinal image, an "artificial eye movement" that consists simply of a constant velocity of about 0.1 deg/s. This stimulus condition is unique: There is no flicker frequency, flash duration, or other form of temporal variation that can mimic the normal contrast sensitivity as well as the solid curve in Fig. 7.

Note that increasing the velocity to 3 deg/s makes low spatial frequencies *more* visible than they are with normal eye movements. This motion is too slow to represent a typical saccade, but retinal image velocities in this range often occur when the *object* is moving. Evidently, the natural drift motions permit us to see both stationary and moving targets with the same type of mechanism, but the spatial tuning of this mechanism varies with the velocity. When the target is stationary, the natural drift keeps it moving with respect to the retina, and hence visible (while the fixational saccades keep it from drifting too far off the fovea).

Saccadic eye movements are probably too fast to stimulate these motion-detecting mechanisms. The data of Fig. 6 indicate that, at velocities greater than 100 deg/s, there would be no contrast sensitivity at any spatial frequency within the range of normal vision (note that the corresponding temporal frequencies are well above fusion). This may partly explain why there is little or no pattern perception during saccades.[23]

The results of this section provide an important new insight into the nature of the unstabilized contrast sensitivity data. The earlier studies mentioned above[4,8,9,11,13,15] all assumed that the unstabilized flicker and contrast stimuli were orthogonal to each other in the spatio-temporal frequency domain, but that is evidently not the case. We have found that the role of eye movements in maintaining the unstabilized contrast sensitivity is much better simulated by a constant, low velocity than by any other form of temporal variation (or by none at all). Since any constant velocity represents a constant ratio of temporal to spatial frequency, the unstabilized contrast-sensitivity data must lie along a *diagonal* in the spatio-temporal frequency domain,[10] and hence they cannot be orthogonal to the uniform-field flicker data.

IV. CONSTANT-VELOCITY CURVE FITTING

Each of the constant-velocity curves in Fig. 6 represents the projection, on the spatial-frequency plane, of a 45° profile across the spatio-temporal threshold surface. A sufficient number of such constant-velocity curves can therefore be used to construct this surface, just as one can use the constant-frequency curves of Kelly,[8] Robson,[9] or Van Nes *et al.*[11] However, these (stabilized) constant-velocity curves all have nearly the same shape, and this greatly simplifies the task of modeling the threshold surface. The large variations of curve shape that occur when the spatial or temporal frequency is held constant (*e.g.*, Figs. 1–4) are not found when the velocity is held constant (at any value greater than about 0.1 deg/s).

We will represent the standard passband obtained at a constant velocity by a template of the form,

$$F(\alpha) = \alpha^2 \exp(-|\alpha|), \tag{4}$$

which the author has used elsewhere to represent the spatial frequency characteristics of retinal receptive fields.[24] Equation (4) was originally introduced on theoretical grounds, which will not be reviewed here. Note, however, that for a

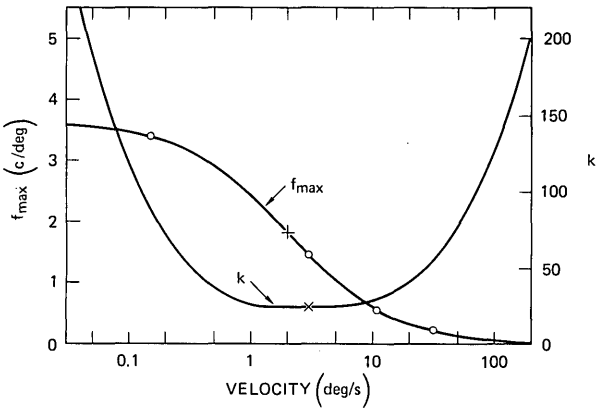

FIG. 8. Graphs of the two scale factors given by Eqs. (6) and (7) as functions of log velocity. Open circles show the peak frequencies ($\alpha_{max}/2\pi$) for the four theoretical contrast-sensitivity curves of Figs. 9 and 10.

constant velocity, its exponential high-frequency flank is consistent with the exponential *square-root* characteristic required by the diffusion model of flicker thresholds,[25] because the two functions are related by a 45° rotation in the spatio-temporal frequency domain.[10]

The main virtue of Eq. (4) in the present context is that, with appropriate scale factors, it provides a reasonably good fit to the stabilized, constant-velocity data for $v > 0.1$ deg/s. The scale factors must both be functions of velocity v, one giving the height, and the other the peak frequency, of the standard passband. It is reasonable to assume that these two parameters vary as well-behaved, smoothly changing functions of velocity, and hence that we can interpolate the results for any velocity within the range of the data.

An expression based on Eq. (4) that fits the data is

$$G(\alpha,v) = kv\alpha^2\exp(-2\alpha/\alpha_{max}), \quad (5)$$

with the two scale factors,

$$k = 6.1 + 7.3\,|\log(v/3)|^3 \quad (6)$$

and

$$\alpha_{max} = 45.9/(v + 2) \quad (7)$$

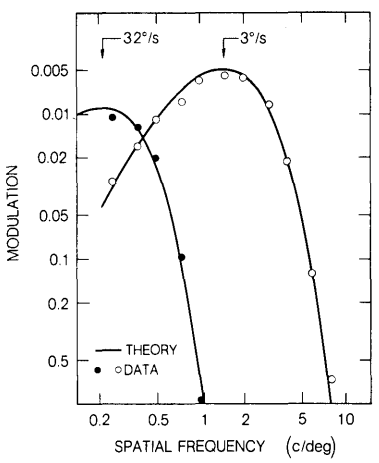

FIG. 9. Graphs of Eq. (5) for $v = 3$ deg/s and $v = 32$ deg/s, with values of k and α_{max} given by Eqs. (6) and (7). The points represent data from Fig. 6 for these two velocities.

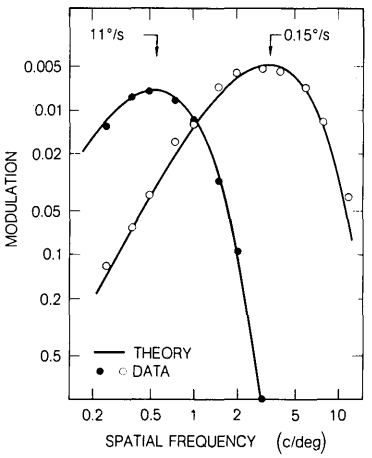

FIG. 10. Graphs of Eq. (5) for $v = 0.15$ deg/s and $v = 11$ deg/s, with values of k and α_{max} given by Eqs. (6) and (7). The points represent data from Fig. 6.

where v is measured in degrees per second, and $\alpha \equiv 2\pi$ (cycles per degree). These three equations represent the model we will use throughout the rest of the paper. They can also be combined, if desired, into the single expression,

$$G(\alpha,v) = [6.1 + 7.3|\log(v/3)|^3] \times v\alpha^2\exp[-2\alpha(v + 2)/45.9]. \quad (8)$$

The exact values of the constants in Eqs. (6) and (7) were obtained by computed-aided, trial-and-error data fitting. In choosing the general forms for these expressions, however, we were guided by several known properties of the spatio-temporal threshold surface. For example, as the spatial frequency decreases, the temporal response curves eventually approach a fixed, asymptotic form (the *Ganzfeld* flicker response). The spatial response also asymptotes in an analogous way as the temporal frequency decreases (if we neglect the fading that occurs at velocities less than 0.1 deg/s). Over the entire range of interest, in fact, the threshold surface exhibits strong spatio-temporal reciprocity. [By substituting ω/α for v, it can be seen that the spatial and temporal frequency variables are almost interchangeable in Eqs. (5)–(8)] Equations (6) and (7) are both plotted in Fig. 8, over a velocity range of 5000 to 1. Note that k is an even function of log velocity, centered at 3 deg/s, while α_{max} is an odd function, centered at 2 deg/s. If both "corner velocities" were exactly the same, the entire spatio-temporal threshold surface would be perfectly symmetric about a diagonal plane located at that velocity.

Figures 9 and 10 show how well this model fits the constant-velocity data. The points in these two figures represent the same contrast thresholds that were given in Fig. 6 but the four curves shown here are theoretical. These curves are plots of $G(\alpha,v)$, as given by Eq. (8), with $v = 32$, 11, 3, and 0.15 deg/s. The result is a reasonably good fit in all four cases (especially in view of the normal variability of such threshold data).

For velocities much greater than 50 deg/s or much less than 0.1 deg/s, this simple model no longer conforms to the data as well as it does in Figs. 9 and 10. However, the velocity range where it does conform well is sufficient to cover all the spatial and temporal frequencies of interest (including those invoked by natural eye movements), so we have not attempted to extend the model further. The velocities used in Figs. 6, 9, and

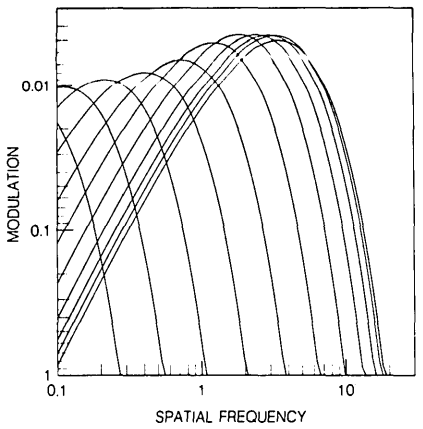

FIG. 11. Theoretical curves of contrast sensitivity at constant velocity obtained from Eq. (5), or (8), for velocities of 0.125, 0.25, 0.5, 1, 2, 4, 8, 16, 32, 64, and 128 deg/s. Note that the peak frequency is inversely proportional to the velocity at high velocities, but becomes approximately constant at low velocities. The entire spatio-temporal threshold surface for traveling waves can be constructed by interpolating between these curves.

10 (and plotted as four points on one of the parametric curves in Fig. 8) were chosen to bracket the desired range.

A more complete family of constant-velocity curves is shown in Fig. 11. These were calculated with equal increments of log velocity, to show how Eq. (7) controls their spatial-frequency tuning. This figure includes the 32 deg/s curve from Fig. 9 and ten other theoretical contrast-sensitivity functions, each representing a velocity that differs from its immediate neighbors by a factor of 2. These velocities range from 0.125 to 128 deg/s.

When the velocity is much greater than 2 deg/s, Eq. (7) makes the peak frequency, α_{max}, inversely proportional to the velocity, so each high-velocity profile is displaced about an octave in spatial frequency. When the velocity is much less than 2 deg/s, Eq. (7) holds α_{max} constant, so the low-velocity profiles tend to be superimposed. At intermediate velocities, there is a smooth transition from one property to the other.

Fig. 11 can be regarded as characterizing the spatio-temporal threshold surface in terms of equally-spaced profiles, all oriented at 45° (in log-log coordinates). Other ways of depicting this surface are considered in Sec. VI.

V. LINE-SPREAD FUNCTIONS

Since the shape of the contrast-sensitivity function at a fixed velocity resembles the Fourier transform of a receptive-field profile, it is of some interest to calculate the inverse transforms of our constant-velocity curves. In accord with recent usage in the psychophysical literature,[19,26–28] we will refer to the one-dimensional transform as a "line-spread function." Because it depends on the temporal properties of the stimulus, however, this concept is quite different from the static line-spread function of optics.

Previous psychophysical line-spread data[26–28] were obtained with spatially localized stimuli of fixed temporal frequency content. Our constant-velocity data were obtained with wide-field stimuli, and yet they appear to represent the behavior of local mechanisms. If we were dealing with microelectrode outputs from a single unit, then it might be possible to predict the response of the cell to a moving line from its responses to sine-wave gratings *moving at the same velocity*, by calculating the one-dimensional Fourier transform of the grating data. But when we apply the same calculation to our wide-field psychophysical thresholds, we could be dealing with a large range of receptive-field sizes,[29] so we would not necessarily expect the result to look like any one of them. And yet it does.

The one-dimensional Fourier transform of our standard contrast-sensitivity function, as in Eq. (4), is

$$f(x) = (2/\pi)(1 - 3x^2)(1 + x^2)^{-3}. \quad (9)$$

By similarly transforming Eq. (8), we can obtain a continuum of line-spread functions like Eq. (9), scaled by the values of k and α_{max}; e.g., we could calculate a line-spread function corresponding to any of the 14 curves in Figs. 9–11. Four of these functions, corresponding to the four sets of contrast-sensitivity data in Figs. 9 and 10, are shown in Fig. 12.

The shapes and sizes of these calculated line-spread functions are in fact similar to those inferred from the psychophysical techniques that use a small, local stimulus.[26–28] For example, the curve shown at (a), which represents a velocity close to the subject's natural drift velocities, has about the same width as the (unstabilized) foveal line-spread function of Wilson[26] or Hines.[28] The other curves, for higher velocities, resemble the wider line-spread functions that have been measured at increasing eccentricities. Electrophysiological measurements show a similar trend: receptive-field size increases with eccentricity.[29]

Our results give no information about eccentricity, of course, except that they must refer to mechanisms within the 7.5° diameter of the drifting stimulus pattern. However, they do suggest a large range of receptive-field sizes and sensitivities (emphasized by the use of linear coordinates in Fig. 12). The widest line-spread function, shown at (d), is about 15 times wider than the narrowest. The height of each central lobe depends inversely on its width, so that the area remains approximately constant[30] (as does the volume, in the case of the point-spread function). This implies that the total background flux integrated by the central lobe of a given re-

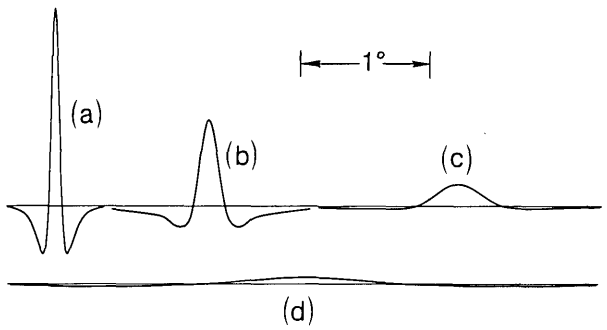

FIG. 12. Line-spread functions derived as the one-dimensional Fourier transforms of the four theoretical curves in Figs. 9 and 10. Both spatial and sensitivity coordinates are linear, emphasizing the large range of sizes invoked by varying the stimulus velocity. The velocities are: (a) 0.15 deg/s, (b) 3 deg/s, (c) 11 deg/s, and (d) 32 deg/s. Note the resemblance to line-spread functions measured psychophysically at various eccentricities (see text).

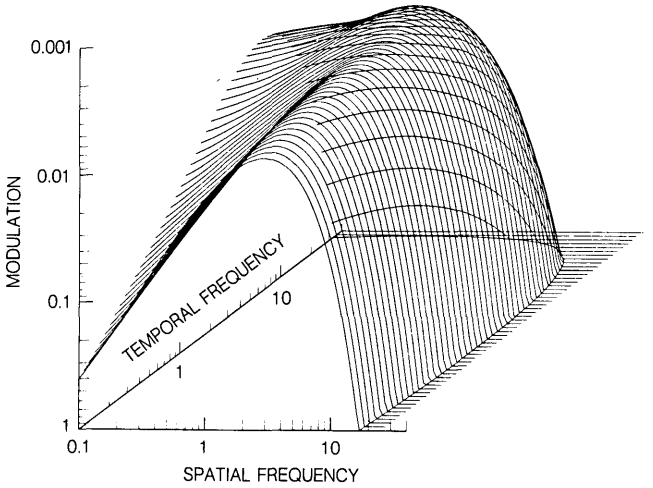

FIG. 13. Perspective view of the spatio-temporal threshold surface for traveling waves, derived from Eq. (8). Each individual curve represents the spatial frequency response at a fixed temporal frequency. The neighboring curves are separated by a constant increment of 0.05 log temporal frequency. (The hidden part of the surface was not suppressed.)

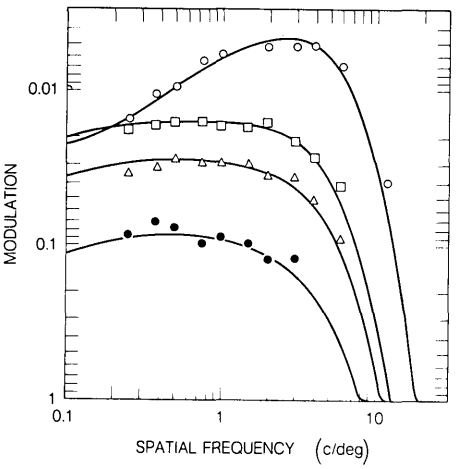

FIG. 14. New contrast-sensitivity data for traveling waves at constant temporal frequencies of 2 Hz (open circles), 13.5 Hz (open squares), 17 Hz (open triangles), and 23 Hz (filled circles). The curves are members of the family shown in Fig. 13.

ceptive field is roughly independent of its size. Some retinal ganglion cells do behave that way, at least in the cat.[31]

Given the assumption of isotropism, the results of Fig. 12 contain no new information that was not present in Figs. 9 and 10. But they do emphasize the point that our psychophysical data behave very much like single-unit responses (although there was no good reason to expect them to). If that is true of the line-spread functions, then it is equally true of the constant-velocity spatial response curves from which they were derived.

VI. THRESHOLD SURFACE

Since the constant-velocity curves completely characterize the spatio-temporal threshold surface, these data can readily be transformed into the usual spatial and temporal frequency coordinates. By programming Eq. (8) into a standard computer graphics package, we can also produce other representations, as desired. Figure 13 is a perspective view of the threshold surface, obtained from such a plotting program.

Each curve in this figure lies in a plane parallel to the spatial frequency axis, and each of these planes differs from its immediate neighbors by an increment of 0.05 log unit (about 12%) along the temporal frequency axis. Hidden regions of the surface are not suppressed, yielding a "transparent" effect. Each of these curves can be regarded as the spatial frequency response for a fixed temporal frequency.

Four members of this family of theoretical contrast-sensitivity curves are shown in Fig. 14, together with some experimental data points obtained for the same subject used in Fig. 6 *et seq.* Since these are new data, their agreement with the model adds weight to the evidence of the previous data comparisons (although it does not, of course, provide a fundamentally different type of test, because the data of Fig. 6 *et seq.* could also be arranged with temporal frequency as the parameter).

Figure 13 provides a qualitative picture of the behavior of the threshold surface, but the same data can be read more accurately from the contour map shown in Fig. 15. Note that the log velocity scale in the upper right corner of this figure is compressed by a factor of $\sqrt{2}$ (due to the 45° rotation). Hence a large velocity range is required to cover much smaller frequency ranges.

The reciprocal relation between the spatial and temporal responses is particularly clear in Fig. 15. The entire surface is almost symmetric, reflected about a "corner velocity" of 2 deg/s, shown by the dashed line on the velocity scale. The heavy line labeled "max" represents the maximum sensitivity

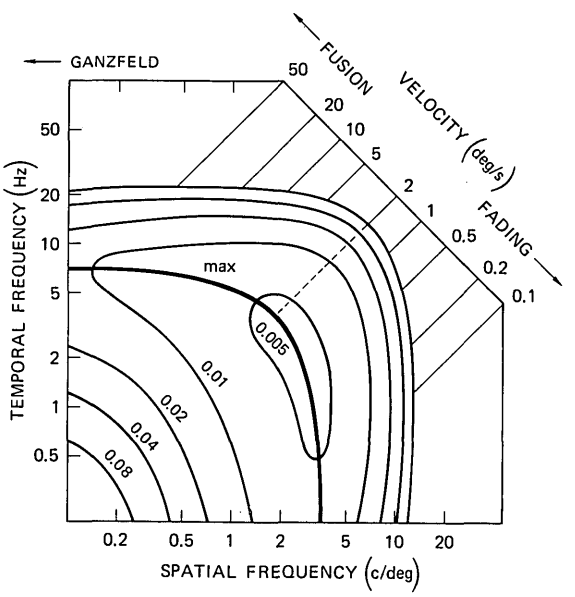

FIG. 15. Contour map of the same spatio-temporal threshold surface given in Fig. 13. Note the scale of velocities in the upper right corner. The heavy line ("max") represents the maximum sensitivity at each velocity. The contours represent equal increments of log sensitivity, as labeled. The map is approximately symmetric about the (dashed) diagonal line, $v = 2$ deg/s.

at each velocity. Where this line runs horizontally, the temporal frequency response is nearly independent of spatial frequency; hence α_{max} must be inversely proportional to the velocity in this region (see Fig. 11). These high velocities are characteristic of fast-moving objects in the environment. Where the "max" line in Fig. 15 runs vertically, the spatial response is nearly independent of temporal frequency; hence, α_{max} doesn't vary with velocity in this region. These low velocities are characteristic of natural drifts that occur when the subject is fixating a stationary object.

The sensitivity is greatest in the intermediate region, reaching its maximum in the vicinity of 2 deg/s. At higher velocities, the sensitivity decreases with increasing velocity, until even a high-contrast target is fused. (Most saccadic velocities fall in this region.) At low velocities, the sensitivity decreases with decreasing velocity; eventually, the target begins to fade out, and may disappear entirely at zero velocity, if the stabilization is precise enough.[1]

Between these two extremes (*i.e.*, in the region of normal vision), the results of Fig. 15 (or Figs. 11 or 13) can predict the visibility of any traveling-wave stimulus under our conditions, which include stabilizer-controlled motion and a 7.5°, 300-td field. Smaller fields or unstabilized viewing produce quite different results,[32] as do other spatial patterns.[33] For counterphase-flickering gratings, however, the threshold surface seems to be identical in shape to the one given here, but depressed in sensitivity by a factor of 2, as shown in Sec. II.

VII. DISCUSSION

This paper marks the completion of a project that began almost 20 years ago, with our first proposals to measure the spatio-temporal threshold surface.[2–4] Now that we have such measurements uncontaminated by eye movements, we can try to account for them in terms of known or plausible properties of the visual pathways.

The ability to substitute precisely controlled proximal stimulation in place of eye movements also provides an important tool for studies of the relation between eye movements and pattern detection. A comparison of Fig. 15 with the contour map recently prepared by Koenderink and Van Doorn[32] from their unstabilized spatio-temporal thresholds shows that eye movements do have important effects on the thresholds for drifting and flickering gratings (a point on which the previous literature was in some disagreement).

Koendrink and Van Doorn[32] found that natural eye movements gave their threshold surface a more complicated shape, splitting the sensitivity peak into two separate maxima. One of these (which they called the "flicker" maximum) was shifted to somewhat lower spatial and higher temporal frequencies, while the other (the "pattern" maximum) appeared at very low temporal frequencies. Since the "pattern" maximum occurred at velocities much less than 0.1 deg/s (where stabilized patterns fade out), it must have been created by natural eye movements, while the "flicker" maximum is evidently a distorted version of the stabilized result.[34] It seems likely that other evidence for the so-called pattern–flicker dichotomy may also be contaminated by similar eye-movement artifacts.

Our results suggest that retinal image motion is the *sine qua non* of vision. If a moving sinusoidal grating is projected on the retina in a way that is not affected by eye movements, it maintains its visibility under conditions where other stimuli vanish. For example, when identical, stationary and moving gratings are superimposed, only the moving one controls the threshold. Similarly, the threshold for a standing-wave stimulus is determined by its traveling-wave components; this relation holds over most of the spatio-temporal frequency domain. The visual process seems to be designed to respond to stimulus velocities within the range shown in Fig. 15. When the image motion needed for these responses is not supplied by the environment, it must be provided by eye movements.

If the stabilized contrast sensitivity is measured at a constant velocity of the grating with respect to the retina, a characteristic spatial-frequency passband is obtained, with peak frequency inversely related to velocity. When this velocity equals the average speed of the subject's natural drift motions, the result is close to his normal, unstabilized contrast sensitivity, which tends to confirm that normal vision is mediated by these drift motions. When the retinal image velocity is increased beyond the normal drift rate, the contrast-sensitivity function moves toward lower spatial frequencies but it maintains the same shape (which resembles the Fourier transform of a receptive-field function). This result again suggests that both stationary and moving targets may be detected by the same type of mechanism, with retinal drift required for stationary targets.

The concept of spatial frequency tuning over a continuous frequency range has been invoked previously to explain the results of complex-waveform[35,36] and pattern-adaption[37] experiments, among others. However, it is not at all clear that our constant-velocity experiments are tapping the same mechanisms as either (or both) of these well-known techniques. Our "channels" are merely diagonal profiles across the spatio-temporal threshold surface, but that is not the way other spatial-tuning experiments[35–37] are usually interpreted. The relation between the results of Fig. 6 and other types of spatial tuning is another important subject for further study.

ACKNOWLEDGMENTS

For the development of our stabilization equipment, the author is indebted to all the colleagues mentioned in Part I. The additional techniques required to move our stimuli at precise, constant velocities under computer control were developed by C. M. Steele. The program that produced Figs. 11 and 13 *et seq.* was written by M. R. Clark. The paper has benefited from insightful comments by C. A. Burbeck. Work was supported by NIH Grant No. EY 01128.

[1] D. H. Kelly, "Motion and vision. I. Stabilized images of stationary gratings," J. Opt. Soc. Am. **69**, 1266–1274 (1979).
[2] D. H. Kelly, "J_0 stimulus patterns for visual research," J. Opt. Soc. Am. **50**, 1115–1116 (1960).
[3] D. H. Kelly, Ph.D. thesis, University of California at Los Angeles (1960) (unpublished).
[4] D. H. Kelly, "New stimuli in vision," in *Abbilden und Sehen*, Proceedings of the 6th meeting of the International Commission for Optics, edited by H. Schober and R. Röhler (Munich, 1962), pp.

119–126.
[5]H. deLange, "Experiments on flicker and some calculations on an electrical analogue of the fovea systems," Physica **18,** 935–950 (1952). See also H. deLange, "Research into the dynamic nature of the human fovea-cortex systems with intermittent and modulated light," J. Opt. Soc. Am. **48,** 777–789 (1958).
[6]O. H. Schade, "Electro-optical characteristics of television systems. I. Characteristics of vision and visual systems," RCA Review **9,** 5–37 (1948).
[7]References 2–4 also proposed the use of circular standing waves, which require two-dimensional analysis. Here we treat only the simpler, one-dimensional case of rectilinear, sine-wave patterns.
[8]D. H. Kelly, "Frequency doubling in visual responses," J. Opt. Soc. Am. **56,** 1628–1633 (1966).
[9]J. G. Robson, "Spatial and temporal contrast sensitivity functions of the visual system," J. Opt. Soc. Am. **56,** 1141–1142 (1966).
[10]In logarithmic coordinates.
[11]F. L. van Nes, J. J. Koenderink, H. Nas, and M. A. Bouman, "Spatiotemporal modulation transfer in the human eye," J. Opt. Soc. Am. **57,** 1082–1088 (1967).
[12]In Ref. 11, horizontal gratings moved vertically, while our vertical gratings moved horizontally. However, there seems to be no evidence of a significant difference between the horizontal and vertical motion thresholds.
[13]E. Levinson and R. Sekular, "The independence of channels in human vision selective for direction of movement," J. Physiol. (Lond.) **250,** 347–366 (1975).
[14]D. H. Kelly, "Visual contrast sensitivity," Opt. Acta **24,** 107–129 (1977); see Fig. 16.
[15]D. H. Kelly, "Adaptation effects on spatio-temporal sine-wave thresholds," Vision Res. **12,** 89–101 (1972).
[16]If the spatial frequency is low enough, the ratio of traveling-wave to standing-wave sensitivity must depend on the phase of the standing wave; e.g., if an antinode of the standing wave fills the visual field, the two sensitivities must be equal. At a node, on the other hand, the standing-wave sensitivity must be zero. Normally the sensitivity ratio falls between these two extreme cases, so there must be some kind of spatial averaging across the standing wave.
[17]Since our flicker and motion signals were derived from different sources, they could not be phase-locked in the present apparatus (see Ref. 1); i.e., we were unable to maintain $v = \omega/\alpha$ exactly. As a result, neither component was perfectly stabilized during this experiment, and the residual destabilization probably increased the thresholds in Fig. 5.
[18]E. M. Levinson (personal communication).
[19]See Ref. 14, Fig. 12.
[20]The zero-velocity data are similar to those given in Ref. 1, Figs. 6–9(d). The question of whether these sustained responses are significantly affected by residual motions in the stabilization apparatus was discussed in Sec. III of Ref. 1.
[21]A. Watanabe, T. Mori, S. Nagata, and K. Hiwatashi, "Spatial sine-wave responses of the human visual system," Vision Res. **8,** 1245–1263 (1968). See their Fig. 11 (but note that some velocities are identified incorrectly in the figure caption).
[22]L. E. Arend, Jr., "Temporal determinants of the form of the spatial contrast threshold MTF," Vision Res. **16,** 1035–1042 (1976). Data are given for three velocities of the fixation point (including zero), in Fig. 5.
[23]R. W. Ditchburn, *Eye-movements and Visual Perception* (Clarendon, Oxford, 1973), p. 367 *et seq*.
[24]D. H. Kelly, "Spatial frequency selectivity in the retina'" Vision Res. **15,** 665–672 (1975).
[25]D. H. Kelly, "Diffusion model of linear flicker responses," J. Opt. Soc. Am. **59,** 1665–1670 (1969).
[26]H. R. Wilson, "Quantitative characterization of two types of line-spread function near the fovea," Vision Res. **18,** 971–981 (1978).
[27]J. O. Limb and C. B. Rubinstein, "A model of threshold vision incorporating inhomogeneity of the visual field," Vision Res. **17,** 571–584 (1977).
[28]M. Hines, "Line spread function variation near the fovea," Vision Res. **16,** 567–572 (1976).
[29]For example, see B. Fischer, "Overlap of receptive field centers and representation of the visual field in the cat's optic tract," Vision Res. **13,** 2113–2120 (1973).
[30]If the maximum sensitivity in Figs. 9 and 10 did not vary with velocity, i.e., if k were exactly constant in Eqs. (5) *et seq.*, this area would be exactly constant.
[31]T. H. Harding and C. Enroth-Cugell, "Absolute dark sensitivity and center size in cat retinal ganglion cells," Brain Res. **153,** 157–162 (1978), summarizes a number of studies by Enroth-Cugell and her collaborators that confirm this conclusion.
[32]J. J. Koenderink and A. J. van Doorn, "Spatiotemporal contrast detection threshold surface is bimodal," Opt. Lett. **4,** 32–34 (1979).
[33]D. H. Kelly and H. S. Magnuski, "Pattern detection and the two-dimensional Fourier transform: Circular targets," Vision Res. **15,** 911–915 (1975).
[34]J. J. Koenderink (personal communications).
[35]F. W. Campbell and J. G. Robson, "Application of Fourier analysis to the visibility of gratings," J. Physiol. (Lond.) **197,** 551–566 (1968).
[36]N. Graham and J. Nachmias, "Detection of grating patterns containing two spatial frequencies: a comparison of single-channel and multiple-channels models," Vision Res. **11,** 251–259 (1970).
[37]C. Blakemore and F. W. Campbell, "On the existence of neurones in the human visual system selectively sensitive to the orientation and size of retinal images," J. Physiol. (Lond.) **203,** 237–260 (1969).